A NEW MATHEMATICAL MODELING OF CONTACT TREATMENT BETWEEN AN ORTHOTROPIC MATERIAL AND A RIGID INDENTER

H. Ashrafi[1,*], M. Mahzoon[2] and M. Shariyat[1]
* *hashrafi@dena.kntu.ac.ir*

[1] Department of Mechanical Engineering, K. N. Toosi University of Technology, Tehran, Iran.
[2] Department of Mechanical Engineering, School of Engineering, Shiraz University, Shiraz, Iran.

Abstract: *The boundary value problems involving contact are of the great importance in industries related to mechanical and materials engineering. These mixed problems are challenging since a priori unknown deformed surface of the material contacting a rigid indenter is to be determined as a part of the solution. Anisotropic solids represent an important class of engineering materials including crystals, woods, bones, thin solid films, polymer composites, etc. Contact analysis of an anisotropic media, however, is more difficult and is developed less completely in the literature. In this work, both analytical and computational studies of the contact treatment of a semi-infinite orthotropic material indented by a rigid spherical indenter have been considered in two different sections. This approach can be applied to determine the interfacial contact area and pressure distribution for three-dimensional orthotropic materials, and can then be used to calculate the resulting stress and strain fields of the media. Results presented herein can serve as benchmarks with which to compare solutions obtained by ANSYS commercial package.*

1. INTRODUCTION

Contact phenomena arise due to interactions between mechanical components, in which most of the mechanical loads result from such interactions. This statement is an indication of the importance of the contact problems in engineering design and analysis, which have been an active research area in recent years. The contact problems, however, are seldom included in conventional engineering design process due to their complex formulations. The complexity in formulation arises due to several aspects, such as: Inherent nonlinearity of the problem essentially due to the unknown contact surface and unknown boundary conditions on this surface during the loading of structure; requiring of the rigorous mathematical foundations for modeling of the interfacial contact; effects of geometric and material nonlinearity and also dynamic nature of some problems. Therefore, the contact problems for even linear elastic materials are challenging because the configuration of the contact zone and the pressure distribution on it are generally unknown a priori. The difficulty of the problem increases with an increase in the degree of anisotropy of the solid material. Orthotropic solids, which their mechanical properties differ

along each of three principal coordinate axes of a Cartesian coordinate system, represent a class of important materials including crystals, woods, biological tissues, etc. [1–2]. Since nine independent elastic constants are needed to define the elastic characteristics of the orthotropic media, the analysis of an orthotropic solid is more complex than other materials.

For many years, researchers have been considering the contact analysis of isotropic solids. Roots of research on the contact phenomenon return into the eighteenth century. During that period of development, the contact bodies were treated as rigid, primarily to keep the formulation simple. However, that approach could not predict the deformations and stresses inside a body. Hertz investigated the elastic contact between two bodies and obtained an analytical solution to describe the stresses and deformations near the contact point [3]. Hertzian contact theory has been considered as an important event in the history of the contact mechanics. A variety of analytical solutions of linear problems for the isotropic materials with different approximations have been summarized by Johnson [3] and Popov [4]. The contact analysis of the orthotropic media is less completely developed in the literature, although

the analytical solutions are available for special cases such as transversely isotropic materials. The contact solutions for the transversely isotropic solids have been presented in several works such as Lekhnitskii [1], Turner [5], Keer and Schonberg [6], Ovaert [7], and Brock et al. [8]. Some approximate solutions have been utilized to investigate the contact problems of orthotropic media. A simple two-dimensional solution is available for the orthotropic solids under transverse pressure loading by Srinivas and Rao [9] and Miller [10]. These solutions have been given in terms of Fourier series expansions of the transverse pressure loading on layered orthotropic solids with simply supported boundary conditions. Based on experimental results, Yang and Sun [11] modified the Hertz contact law for an orthotropic layer by assuming that the pressure distribution on the contact surface and the width of the contact zone for an anisotropic layer can be calculated from those for an isotropic one by replacing Young's modulus by the elastic modulus of the anisotropic layer in the indentation direction. Wu and Yen [12], and Chao and Tu [13] used Green's function to investigate the contact between a simply supported orthotropic plate and a rigid sphere, and then numerically associated the resulting surface displacements to indenter geometry. A simple finite-element study of the contact behavior of laminated beams has been carried out by Mahajan [14], who studied the influence of various parameters such as beam thickness, indenter size, presence of a compliant layer and the presence of delamination on the contact behavior of a symmetric orthotropic laminate.

Moreover, Fan et al. [15] investigated the effect of elastic anisotropy on indentation measurements in human tibial cortical bones. They developed a theoretical analysis of indentation for an orthotropic media to quantitatively predict the indentation modulus using stiffness matrix that was obtained from experimental results. A numerical analysis of the contact problems has been presented by Shi et al. [16] for the orthotropic media, in which the analysis of indentation by a rigid ellipsoidal indenter against an orthotropic half-space was derived from stress equilibrium. Kagadii and Pavlenko [17] discussed the friction problem on a rigid flat-based die forced into an orthotropic half-strip, whose semi-infinite sides were fixed and the principal axes of anisotropy coincide with the Cartesian coordinate axes. Delafargue and Ulm [18] solved explicitly the elastic contact problems between an axisymmetric indenter and a general orthotropic semi-infinite solid in closed form. They proposed an explicit solution for the indentation moduli of a transversely isotropic medium and a general orthotropic medium under rigid conical indenter in three principal material symmetry directions, in which the half-space Green's functions were interpolated from their exact extreme values. Swanson [19] used Willis's method [20] of double Fourier transforms to reduce governing coupled partial differential equations for the three displacement components to ordinary differential equations which involve derivatives with respect to the coordinate in the indentation direction throughout the interfacial contact region of generally orthotropic finite thickness plates. Fukumasu and Souza [21] conducted a series of finite element analyses to simulate the indentation of systems with an elastic film and an elastic-plastic substrate. They indicated that the amount of substrate pile-up and, consequently, the peak in radial stresses at film surface, could be significantly reduced in coated systems with substrates with orthotropic plastic properties. A parameterized orthotropic constitutive model of cancellous bone was derived from three-dimensional finite element analysis of repeatable microstructure cells by Kowalczyk [22]. Lovell and Morrow [23] have used the finite element method to analyze three-dimensional deformations and indentation depths of a spherical indenter normally loaded between two flat layers made of transversely isotropic materials. Kahya et al. [24] considered a frictionless contact problem for a two-layer orthotropic elastic medium loaded through a rigid flat stamp. They assumed that the tensile tractions were not allowed and only compressive tractions can be transmitted across the contact interface, and the problem was expressed in terms of a singular integral equation by using the theory of elasticity and the Fourier transforms. Batra and Jiang [25] used Stroh's formalism [26] to analytically study the generalized plane strain deformations of a linear elastic orthotropic layer bonded to a rigid substrate, and

indented by a rigid cylindrical indenter. They presented a parametric study to describe the effect of various material and geometric parameters upon the load required to indent an orthotropic layer by a prescribed amount. Ashrafi and Farid [27-28] developed a relation between the resultant indentation force, the contact pressure distribution and the penetration into an orthotropic viscoelastic layer using a matrix inversion method with exactly satisfying the boundary conditions.

In this work, a contact problem for a semi-infinite orthotropic medium indented by a rigid sphere is considered. Here, we adopt an analytic solution as well as a numerical modeling to study infinitesimal deformations of an anisotropic solid with the aim of deriving a relation between applied load and indentation depth. In the analytic approach, a mathematical procedure is developed for calculating the contact stresses due to interfacial loading, which can be obtained in a mechanical system. In this solution, a numerical integration is used to calculate the size and aspect ratio of the contact area, the contact pressure distribution and then the stress fields. The unknown constants in the Fourier series are determined by satisfying boundary conditions in an average sense. Afterwards, a numerical analysis is presented with a computer simulation in ANSYS using a finite element model. This investigation describes the behavior of the semi-infinite orthotropic medium concerning the indentation procedure using a computational model in ANSYS. The problem of indentation by a smooth spherical indenter is examined for special orthotropic media. The comparison of results indicates that a good accuracy for solutions can be achieved. The results show that the interfacial area of contact has an elliptical shape for the orthotropic solids under a contact loading by a rigid spherical indenter. Furthermore, the distributions of stress and strain fields significantly differ from an isotropic medium.

2. ANALYTICAL SOLUTION OF THE PROBLEM

The problem studied, as shown schematically in Fig. 1, involves a linear elastic, homogeneous and semi–infinite orthotropic medium indented by a rigid spherical indenter. In many applications
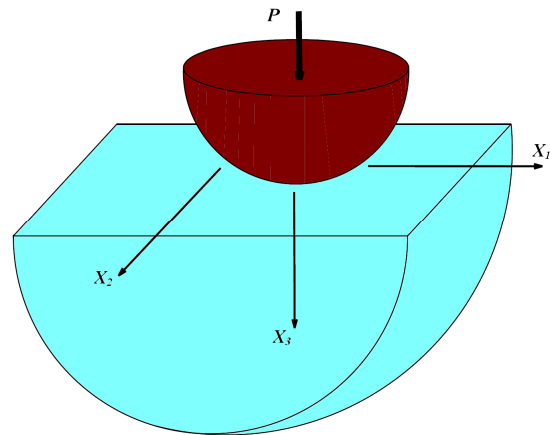

Fig. 1. The schematic geometry of orthotropic indentation

Young's modulus of the indenter is significantly higher than that of the material of the elastic media being indented, and the indenter can be regarded as rigid. When indentation depth is small in comparison to the thickness of the deformable medium, the radius of the indenter, and the width of the medium, the response of the material of the layer may be regarded as linear elastic. We assume that the indentation depth is such as to induce infinitesimal deformations of the material. As the indenter is pressed quasistatically into the linear elastic medium, points of the medium underneath the medium move vertically down, those not on the axis of the indenter also move axially outwards while those near the free surface of the medium and adjacent to the rigid indenter move upwards [25].

Consider that x_3 (or z) direction is normal to the surface of the semi–infinite orthotropic medium. The stress–strain relationship for a solid can be written as [1]:

$$\{\sigma\} = [C]\{\varepsilon\} \tag{1}$$

The eighty–one stiffness constants are needed to relate the stress and strain. Since $\sigma_{ij} = \sigma_{ji}$ and $\varepsilon_{ij} = \varepsilon_{ji}$, the number of material constants needed is reduced to thirty–six. By using the material symmetry, only twenty–one stiffness constants are necessary to describe the most general anisotropic solids. For an orthotropic material, the elastic properties are symmetric in three orthogonal planes; only nine stiffness constants therefore are required.

The stress–strain relationship for an orthotropic semi–infinite medium can be written as:

$$\begin{Bmatrix} \sigma_{11} \\ \sigma_{22} \\ \sigma_{33} \\ \sigma_{23} \\ \sigma_{31} \\ \sigma_{12} \end{Bmatrix} = \begin{bmatrix} C_{11} & C_{12} & C_{13} & 0 & 0 & 0 \\ C_{21} & C_{22} & C_{23} & 0 & 0 & 0 \\ C_{31} & C_{32} & C_{33} & 0 & 0 & 0 \\ 0 & 0 & 0 & C_{44} & 0 & 0 \\ 0 & 0 & 0 & 0 & C_{55} & 0 \\ 0 & 0 & 0 & 0 & 0 & C_{66} \end{bmatrix} \begin{Bmatrix} \varepsilon_{11} \\ \varepsilon_{22} \\ \varepsilon_{33} \\ 2\varepsilon_{23} \\ 2\varepsilon_{31} \\ 2\varepsilon_{12} \end{Bmatrix} \quad (2)$$

where $C_{12} = C_{21}$, $C_{13} = C_{31}$ and $C_{32} = C_{23}$.

The strains are related to the displacements through the strain–displacement relationship as:

$$\varepsilon_{ij} = \tfrac{1}{2}\left\{ u_{i,j} + u_{j,i} \right\} \quad (3)$$

The stress equilibrium equations are written as:

$$\begin{aligned} \sigma_{11,1} + \sigma_{12,2} + \sigma_{13,3} &= 0 \\ \sigma_{21,1} + \sigma_{22,2} + \sigma_{23,3} &= 0 \\ \sigma_{31,1} + \sigma_{32,2} + \sigma_{33,3} &= 0 \end{aligned} \quad (4)$$

By substituting Equations (2) and (3) into the stress equilibrium relations of an orthotropic medium, we have:

$$\begin{aligned} C_{11}u_{1,11} + C_{66}u_{1,22} + C_{55}u_{1,33} + (C_{12}+C_{66})u_{2,12} + (C_{13}+C_{55})u_{3,13} &= 0 \\ C_{22}u_{2,22} + C_{66}u_{2,11} + C_{44}u_{2,33} + (C_{12}+C_{66})u_{1,12} + (C_{23}+C_{44})u_{3,23} &= 0 \\ C_{33}u_{3,33} + C_{55}u_{3,11} + C_{44}u_{3,22} + (C_{13}+C_{55})u_{1,13} + (C_{23}+C_{44})u_{2,23} &= 0 \end{aligned} \quad (5)$$

By taking Fourier transforms of Equations (5) with respect to x and y gives:

$$\begin{aligned} (\omega_1^2 C_{11} + \omega_2^2 C_{66})\tilde{u}_1 - C_{55}\tilde{u}_{1,33} + \omega_1\omega_2(C_{12}+C_{66})\tilde{u}_2 + i\omega_1(C_{13}+C_{55})\tilde{u}_{3,3} &= 0 \\ (\omega_2^2 C_{22} + \omega_1^2 C_{66})\tilde{u}_2 - C_{44}\tilde{u}_{2,33} + \omega_1\omega_2(C_{12}+C_{66})\tilde{u}_1 + i\omega_2(C_{23}+C_{44})\tilde{u}_{3,3} &= 0 \\ C_{33}\tilde{u}_{3,33} - (\omega_1^2 C_{55} + \omega_2^2 C_{44})\tilde{u}_3 - i\omega_1(C_{13}+C_{55})\tilde{u}_{1,3} - i\omega_2(C_{23}+C_{44})\tilde{u}_{2,3} &= 0 \end{aligned} \quad (6)$$

in which Fourier transform can be defined as [29–30]:

$$\tilde{f}(\omega) = \frac{1}{\sqrt{2\pi}} \int_{-\infty}^{+\infty} f(x)\, e^{(i\omega x)}\, dx \quad (7)$$

In this work, the solution is assumed as:

$$\begin{Bmatrix} \tilde{u}_1 \\ \tilde{u}_2 \\ \tilde{u}_3 \end{Bmatrix} = \begin{bmatrix} A_1 \\ A_2 \\ A_3 \end{bmatrix} e^{(ipz)} \quad (8)$$

Firstly, the solutions (8) are substituted into Equations (6), and then by setting the determinant of the derived coefficient matrix to zero, we have:

$$\begin{aligned} p^6 + (f_1\omega_1^2 + f_2\omega_2^2)p^4 + (f_3\omega_1^4 + f_4\omega_1^2\omega_2^2 + f_5\omega_2^4)p^2 \\ + (f_6\omega_1^6 + f_7\omega_1^4\omega_2^2 + f_8\omega_1^2\omega_2^4 + f_9\omega_2^6) = 0 \end{aligned} \quad (9)$$

in which the stiffness constants f_i are represented as follows:

$$\begin{aligned} f_1 &= b_1 + b_3 + b_5 - b_8^2; \quad f_2 = b_2 + b_4 + b_6 - b_9^2 \\ f_3 &= b_1 b_3 + b_1 b_5 + b_3 b_5 - b_3 b_8^2 \\ f_4 &= b_2 b_3 + b_1 b_4 + b_2 b_5 + b_4 b_5 + b_1 b_6 + b_3 b_6 + 2 b_7 b_8 b_9 - (b_4 b_8^2 + b_1 b_9^2 + b_7^2) \\ f_5 &= b_2 b_4 + b_2 b_6 + b_4 b_6 - b_2 b_9^2; \quad f_6 = b_1 b_3 b_5 \\ f_7 &= b_2 b_3 b_5 + b_1 b_4 b_5 + b_1 b_3 b_6 - b_5 b_7^2 \\ f_8 &= b_2 b_4 b_5 + b_2 b_3 b_6 + b_1 b_4 b_6 - b_6 b_7^2; \quad f_9 = b_2 b_4 b_6 \end{aligned} \quad (10)$$

where

$$\begin{aligned} b_1 &= \frac{C_{11}}{C_{55}}; \quad b_2 = \frac{C_{66}}{C_{55}}; \quad b_3 = \frac{C_{66}}{C_{44}} \\ b_4 &= \frac{C_{22}}{C_{44}}; \quad b_5 = \frac{C_{55}}{C_{33}} \\ b_6 &= \frac{C_{44}}{C_{33}}; \quad b_7 = \frac{(C_{12}+C_{66})}{C_{55}} \\ b_8 &= \frac{(C_{13}+C_{55})}{C_{55}}; \quad b_9 = \frac{(C_{44}+C_{23})}{C_{44}} \end{aligned} \quad (11)$$

It should be noted that the final Equation (9) has six roots for p. Therefore the resulting transformed displacements can be given as:

$$\begin{Bmatrix} \tilde{u}_1 \\ \tilde{u}_2 \\ \tilde{u}_3 \end{Bmatrix} = \sum_{k=1}^{6} \begin{bmatrix} (A_1/A_3)_k \\ (A_2/A_3)_k \\ 1 \end{bmatrix} A_{3k}\, e^{(i p_k z)} \quad (12)$$

Six sets of material constants are derived from the prescribed boundary conditions of a semi–infinite orthotropic medium. Three constants of them are determined from the traction-free boundary conditions on the surface of media, which they are:

$$\begin{aligned} \sigma_{13}(x,y,0) &= 0 \\ \sigma_{23}(x,y,0) &= 0 \\ \sigma_{33}(x,y,0) &= -\delta(x)\delta(y) \end{aligned} \quad (13)$$

Consequently, we have:

$$\begin{aligned} \sum_{k=1}^{3}\left[p_k\left(A_1/A_3\right)_k - \omega_1 \right] A_{3k} &= 0 \\ \sum_{k=1}^{3}\left[p_k\left(A_2/A_3\right)_k - \omega_2 \right] A_{3k} &= 0 \\ \sum_{k=1}^{3}\left[C_{13}\,\omega_1\left(A_1/A_3\right)_k + C_{23}\,\omega_2\left(A_2/A_3\right)_k - C_{33}\,p_k \right] A_{3k} &= \frac{-i}{2\pi} \end{aligned} \quad (14)$$

The solution, therefore, is obtained for the transformed displacement fields in terms of parameters ω_1 and ω_2. In addition, the displacement fields should be finite far from the source load, which indicates that only the roots with positive imaginary parts should be obtained.

In a contact problem, two bodies are considered that pressing together so that a resultant contact pressure P between them is created and so there is an interfacial contact over a small area of the surface of each. The orthotropic bodies are assumed to be smooth so that there is only a normal pressure between them. Let contact point be in origin of the systems of Cartesian coordinates (x, y, z_1) and (x, y, z_2), which is chosen so that $x – y$ plane is a common tangent plane and also z_1– and z_2 – axis are directed along the internal normal vectors of the bodies. Afterwards Equations of the surfaces of the orthotropic bodies are given locally as:

$$z_1 = A_1 x^2 + B_1 y^2 + 2H_1 x y$$
$$z_2 = A_2 x^2 + B_2 y^2 + 2H_2 x y \qquad (15)$$

It is assumed that the sum of these quadratic forms is positive definite. After the bodies are pressed together, the displacement fields (u_1, v_1, w_1) and (u_2, v_2, w_2) are produced in them. The relative displacement is supposed that at the origin is δ. Therefore at all points of the contact area between the indenter and body, we have:

$$w_1 + w_2 = \delta - (A x^2 + B y^2 + 2H\, xy) \qquad (16)$$

where

$$A = A_1 + A_2$$
$$B = B_1 + B_2 \qquad (17)$$
$$H = H_1 + H_2$$

On the basis of Hertz solution, Willis [20] conditionally assumed and afterwards proved that the area of contact has an elliptical shape with semi – axes a_1 and a_2. Distribution of the contact pressure was assumed as:

$$p(x,y) = p_0 \left(1 - \frac{x^2}{a_1^2} - \frac{y^2}{a_2^2} \right)^{0.5} \qquad (18)$$

The surface displacement u_3 for a body can be written as:

$$u_3(x,y,0) = \iint_S p_0 \left(1 - \frac{\bar{x}^2}{a_1^2} - \frac{\bar{y}^2}{a_2^2} \right)^{0.5} w(x-\bar{x}, y-\bar{y})\, d\bar{x}\, d\bar{y} \qquad (19)$$

in which $w(x, y) \equiv u_3(x, y, 0)$ and S represents the contact area. By substituting the inverse Fourier transform of the surface displacement w into Equation (19), we have:

$$u_3(x,y,0) = \frac{1}{2\pi} \iint_S p_0 \left(1 - \frac{\bar{x}^2}{a_1^2} - \frac{\bar{y}^2}{a_2^2} \right)^{0.5}$$
$$\left(\int_{-\infty}^{+\infty} \int_{-\infty}^{+\infty} \tilde{w}(\omega_1,\omega_2) e^{-i[\omega_1(x-\bar{x})+\omega_2(y-\bar{y})]}\, d\omega_1 d\omega_2 \right) d\bar{x}\, d\bar{y} \qquad (20)$$

We can reduce this relation to a following integral equation:

$$u_3(x,y,0) = p_0 \frac{\pi a_2}{4} \int_0^{2\pi} \left(1 - \left(\frac{\eta_1 x}{a_1} - \frac{\eta_2 y}{a_2} \right)^2 \right) \tilde{w}(e\eta_1, \eta_2)\, d\theta \qquad (21)$$

where

$$e = a_2 / a_1$$
$$\eta_1 = \cos\theta \quad \eta_2 = \sin\theta \qquad (22)$$

Also the contact force is related to the maximum contact pressure by:

$$F = \frac{2\pi}{3} p_0 a_1 a_2 \qquad (23)$$

For a semi – infinite orthotropic solid and in the case of a rigid indenter, which the axis of the elliptical contact area is aligned with the orthotropic axes, we have:

$$A = \frac{1}{2R_1} = \frac{3F I_1}{8a_1^3}$$
$$B = \frac{1}{2R_2} = \frac{3F I_2}{8a_1 a_2^2} \qquad (24)$$
$$\delta = \left(\frac{3F}{4\sqrt{R_1}} \right)^{2/3} \left(\frac{I_3}{2 I_1^{1/3}} \right) = \frac{3F I_3}{8a_1}$$

in which

$$I_1 = \int_0^{2\pi} \tilde{w}(e\eta_1, \eta_2)\, \eta_1^2 d\theta;$$
$$I_2 = \int_0^{2\pi} \tilde{w}(e\eta_1, \eta_2)\, \eta_2^2 d\theta; \qquad (25)$$
$$I_3 = \int_0^{2\pi} \tilde{w}(e\eta_1, \eta_2)\, d\theta$$

Considering the Equations (24) for a rigid spherical indenter, the size of elliptical contact

area and the indentation depth can be written as:

$$a_1 = I_1^{1/3}\left(\frac{3RF}{4}\right)^{1/3}$$

$$a_2 = \frac{I_2^{1/2}}{I_1^{1/6}}\left(\frac{3RF}{4}\right)^{1/3} \qquad (26)$$

$$\delta = \frac{I_3}{2I_1^{1/3}}\left(\frac{3F}{4\sqrt{R}}\right)^{2/3}$$

At last we can write a numerical algorithm for analytical solution of the problem as follows:

I. Select a starting value for the axis ratio (e).
II. Compute the integrals I_1 and I_2.
III. Determine a new value from the axis ratio (e) by following relation:

$$\frac{I_2}{I_1} = e^2 \frac{R_1}{R_2} \qquad (27)$$

Then this value is used in step I, and steps I – III are repeated until the analytical solution for the ratio (e) converges.
IV. Once a converged value of the ratio (e) is obtained, the complete solution can be obtained then by computing I_3.
V. Determine the contact area and the indentation depth for a given contact force.

By selecting a body that is large in x and y directions and thick in z direction with respect to the size of contact area, the solution can be applied to approximate the pressure loading of a semi – infinite orthotropic solid. In this solution, the displacement fields are obtained in terms of products of Fourier series in x and y directions and exponentials in z direction as:

$$u_{ij}(x,y,z) = \left[\sum_{k=1}^{3} A_{ijk}e^{s_k \cdot z} + \right. \left.\sum_{k=4}^{6} A_{ijk}e^{-s_{k-3}\cdot z}\right]\cos\left(\frac{ix\pi}{a}\right)\sin\left(\frac{jy\pi}{b}\right) \qquad (28)$$

The terms with positive exponentials give rise to numerical difficulties, and limit the number of terms that can be taken in the Fourier series [19].

By introducing a new parameter (($\lambda = h - z$)) and substituting it in Equation (28), the solution can be written as:

$$u_{ij}(x,y,z) = \left[\sum_{k=1}^{3} \overline{A}_{ijk}e^{-s_k \cdot \lambda} + \right. \left.\sum_{k=4}^{6} A_{ijk}e^{-s_{k-3}\cdot z}\right]\cos\left(\frac{ix\pi}{a}\right)\sin\left(\frac{jy\pi}{b}\right) \qquad (29)$$

where

$$\overline{A}\,e^{-s\cdot\lambda} = A\,e^{s\cdot h}e^{-s\cdot\lambda} = A\,e^{s\cdot(h-\lambda)} = A\,e^{s\cdot z} \qquad (30)$$

Therefore terms with negative exponentials are only entered in the solution. The strain fields are obtained from derivatives of the displacement fields, by considering that ($d/dz = d/d\lambda$). The stress fields are finally related to the strain fields by the stress–strain law. Based on the stated equations, we have developed a computer code in MATLAB to solve the problem. As described in the following section, the code has been verified by comparing computed results for two problems with results of finite element solution.

3. FINITE ELEMENT SOLUTION OF THE PROBLEM

Currently many finite element models for the semi – infinite orthotropic media exist. A finite element model is superimposed on the geometrical one; then material properties are assigned and loading conditions are prescribed. Afterwards, the needed analysis is performed. Depending on the level of sophistication of the software used and the requirements of the specific research, the geometry and the finite element mesh are more or less detailed and accurate. In this work, a three-dimensional computer simulation is realized in ANSYS concerning the indentation procedure. The continuum description appears to work well for this procedure. Here a suitable surface to surface contact model between an orthotropic semi – infinite solid and a rigid spherical indenter is considered using a finite element analysis.

A mesh with tetrahedral structural elements is used in all simulations by SOLID187. This element is a higher order three-dimensional, 10-
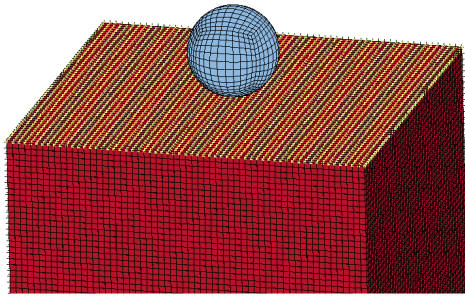
Fig. 2. The finite element mesh model

node element. The element has a quadratic displacement behavior and is well suited to modeling irregular meshes. The element is defined by 10 nodes having three degrees of freedom at each node: translations in the nodal x, y, and z directions. In addition to the nodes, the element input data includes the orthotropic or anisotropic material properties. The orthotropic and anisotropic material directions correspond to the element coordinate directions. Mesh refinements were included to better represent the contact treatment between the rigid indenter and the semi – infinite solid. Three different mesh densities were used in the interfacial area between the orthotropic material and indenter. Fig. 2 schematically illustrates the finite element mesh density and boundary conditions, where fixed boundary conditions are applied along the vertical surfaces of the orthotropic body.

An important contact algorithm, i.e. the augmented Lagrange method, is used for this analysis. This method is basically the penalty method with additional penetration control. This algorithm requires contact normal stiffness, maximum allowable penetration, and maximum

allowable slip. The contact normal stiffness can be derived based on the maximum allowable slip and the current normal contact force. Default normal contact stiffness is provided in ANSYS, which is based on the effective Young's modulus and the size of the underlying elements. If Young's modulus is not found, $E = 1 \times 10^9$ will be assumed. We override the default normal contact stiffness by defining a scaling factor. If a large value is specified for the maximum allowable penetration, the augmented Lagrange method works as the penalty method. For more information about the procedure of numerical analysis for contact problems, you can consider particularly the references [31–32].

4. APPLIED RESULTS AND DISCUSSION

In this section, for validating the accuracy and the efficiency of the proposed approach, the following two numerical orthotropic problems have been used.

Problem 1 – Contact treatment in orthotropic carbon/epoxy materials

The orthotropic solid considered in this study is made up of a laminate consisting of various numbers of 0º and 90º plies of a carbon/epoxy material. The orthotropic properties of a carbon/epoxy material are given in Table 1. The orthotropic properties are then calculated for other layups using a standard lamination theory. The properties are then averaged through the thickness and a single equivalent orthotropic material is being considered. Following the solution algorithm described before, gives a final converged value of ($e = 1.088$). At first, we have plotted the load versus the indentation depth curves for a spherical indenter in Figure 3. In

Table 1. Material properties of an orthotropic carbon/epoxy medium

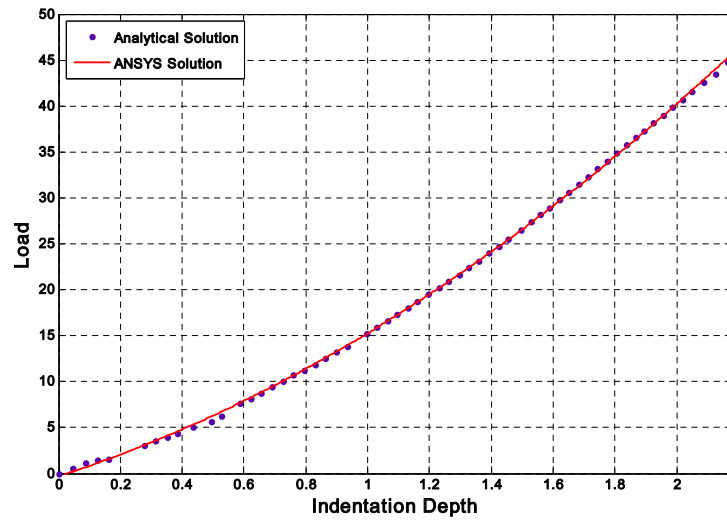| Elasticity Modulus	Values (GPa)	Shear Modulus	Values (GPa)	Poisson's Ratio	Values
E_{11}	130	G_{12}	6.6	v_{21}	0.025
E_{22}	11	G_{13}	6	v_{31}	0.028
E_{33}	12	G_{23}	6	v_{32}	0.33

Fig. 3. Load vs. indentation depth curves for indentation of the orthotropic carbon/epoxy material
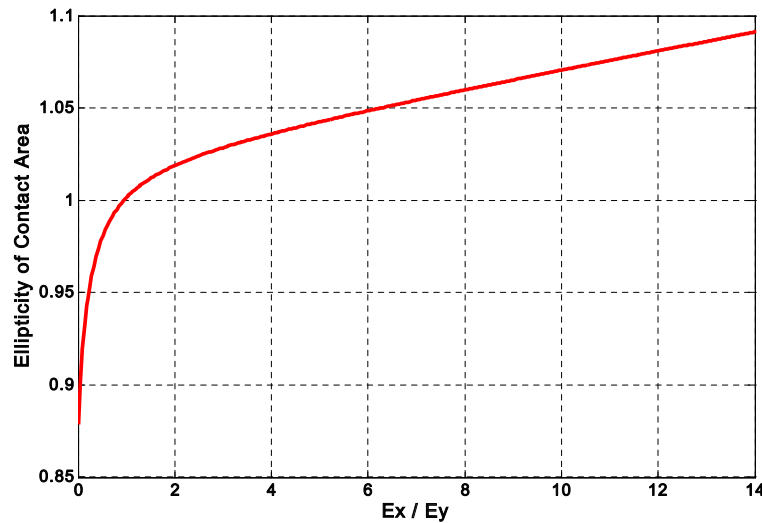

Fig. 4. The elliptic treatment of contact area between bodies

indentation procedures, these curves are used to determine the material properties of the indented sample. There is a good agreement between the analytical results and the numerical results as can be observed in Figure 3.

In addition, Figure 4 shows the axes ratio of the elliptical contact area, (a_2/a_1), as a function of the ratio of in-plane moduli. It should be noted that even with properties as directional as used in this application, with $(E_x/E_y \approx 12)$, the difference between the major and minor axes of the elliptical contact area is about 9 %.

An illustration of the surface displacements calculated by this approach is shown in Figure 5, along with the profile of the spherical indenter. It can be observed that the surface displacement fields for the orthotropic material calculated in the contact area agree very well with the indenter profile.

All stress and strain field are readily calculated by the presented solution. However, the surface normal strain fields in the x and y directions as an example are plotted in Figure 6 versus x and y directions, respectively. You can see a good agreement between the analytical results with those obtained by finite element analysis. It should be noted that since this problem is not
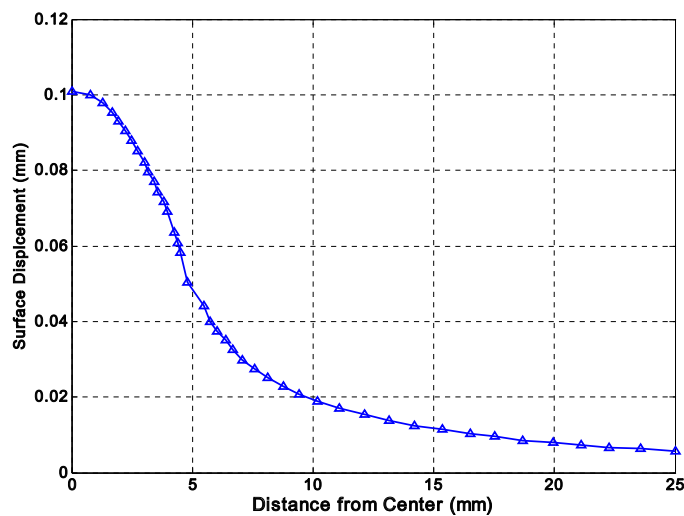
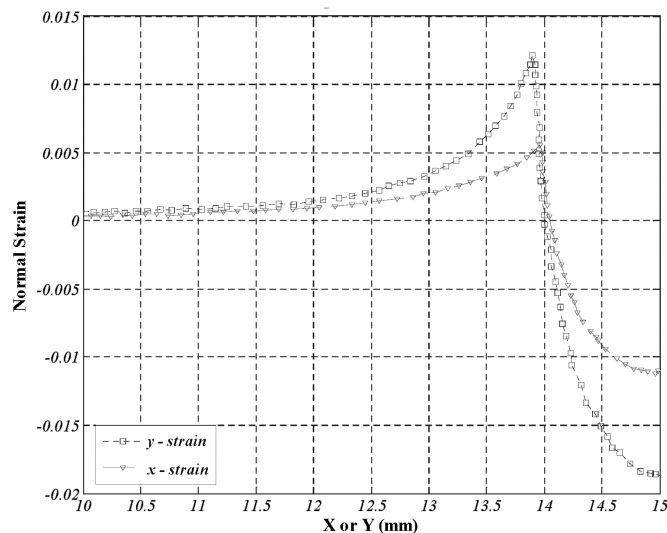**Fig. 5.** The surface displacement field of the carbon/epoxy material

Fig. 6. Normal strain on loaded surface along x and y axis, which center of contact area is at x = y = 15 mm

symmetric, these normal strain fields are different from each other. In addition Fig. 7 illustrates the Von Misses equivalent stress distribution between the rigid indenter and the orthotropic body in ANSYS.

Problem 2 – Contact treatment in orthotropic cortical bones

Another orthotropic solid considered in this study is an orthotropic cortical bone of bovine femur. The orthotropic material properties of a cortical bone are given in Table 2. The aim of the present study is to utilize in vitro the anisotropic elastic properties of the cortical bones.

The cortical bone is a dense, solid compact tissue constituting the diaphyses of long bones and outer shell of the metaphyses mass with only microscopic channels. Approximately 80 % of the skeletal mass in the adult human skeleton is cortical bone, which forms the outer wall of all bones and is largely responsible for the supportive and protective function of the skeleton [33]. The bulk of cortical bone is in the shaft of long bones of the appendicular skeleton. In general, a cortical bone exhibits anisotropic elastic modulus in different anatomic directions. For example, the elastic modulus in the
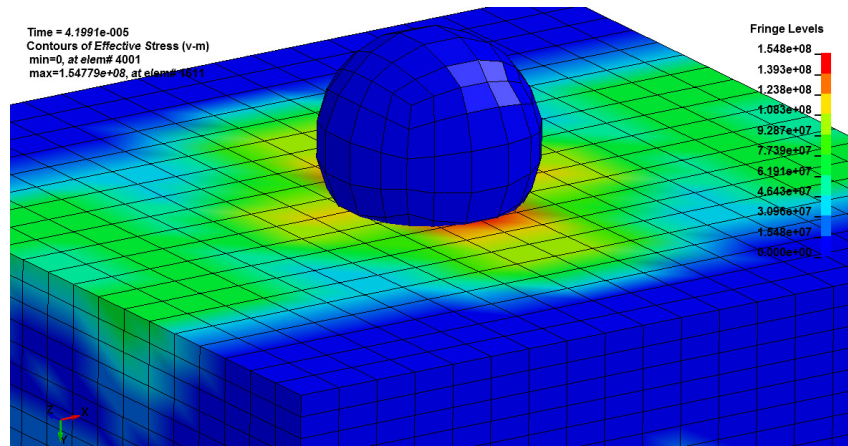
Fig. 7. Von Misses equivalent stress distribution in the carbon/epoxy material

longitudinal direction of long bone is larger than that in the transverse direction. An orthotropic or transversely isotropic constitutive relation describes the cortical bone elastic properties fairly well [33]. One useful method in measuring the elastic properties of a cortical bone is ultrasonic technique. The advantage of ultrasonic method is that the fully anisotropic elastic properties of bone tissue can be determined in a same specimen by propagating ultrasonic waves along different direction of the specimen. The orthotropic properties of the cortical bone of bovine femur are identified by means of an ultrasonic technique as shown in Table 2.

A final converged value of ($e = 1.069$) is achieved following the solution algorithm described before. It should be noted that the difference between the major and minor axes of the elliptical contact area is about 7 %. At first, we have plotted the load versus the indentation depth curves for a spherical indenter in Figure 8. In indentation procedures, these curves are used to determine the material properties of the

indented sample. There is a good agreement between the analytical results and the numerical results as can be observed in Figure 8. You can see a good agreement between the analytical results with those obtained by finite element analysis.

An illustration of the surface displacements calculated by this approach is shown in Figure 9, along with the profile of the spherical indenter. It can be observed that the surface displacement fields for the orthotropic material calculated in the contact area agree very well with the indenter profile. As before example, all stress and strain field are readily calculated by the presented solution. However, the normal strain field in the y direction as an example is plotted in Figure 10. Moreover Figure 11 illustrates the Von Misses equivalent stress distribution between the rigid indenter and the orthotropic body in ANSYS.

5. CONCLUDING REMARKS

A reasonable approximation of several real

Table 2. Material properties of an orthotropic cortical bone

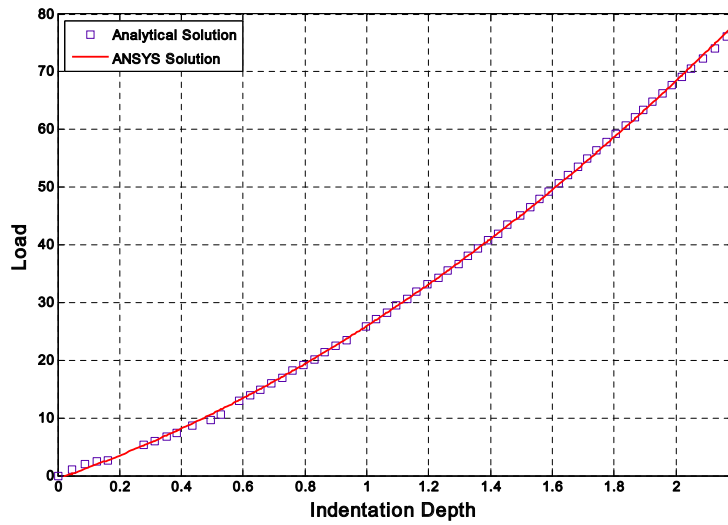| Elasticity Modulus	values (GPa)	Shear Modulus	values (GPa)	Poisson's Ratio	values
E_{11}	20.6	G_{12}	3	v_{21}	0.21
E_{22}	23.4	G_{13}	3	v_{31}	0.29
E_{33}	30.2	G_{23}	4.6	v_{32}	0.24

Fig. 8. Load vs. indentation depth curves for indentation of the orthotropic cortical bone
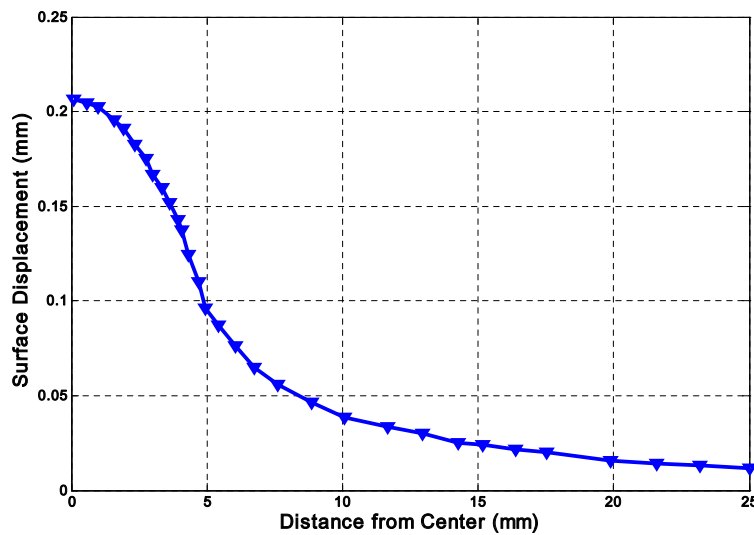

Fig. 9. The surface displacement field of the cortical bone

materials such as crystals and bones is to consider those as an orthotropic linear elastic solid governed by the Hooke's law. In this study, we established an analytical solution to study infinitesimal deformations of an anisotropic solid with the aim of deriving a relation between applied load and indentation depth. A general procedure for numerical integrating of integral equations has been developed to determine the size and the aspect ratio of elliptical contact area. The detailed stress fields are then obtained by these parameters in the general solution for the

orthotropic solids. In addition, a numerical simulation and analysis of contact problems of an orthotropic half space which indented by a rigid spherical indenter, has been considered using a finite element code in ANSYS. The comparisons of results for two special cases indicate that a good accuracy of the solution has been achieved for the orthotropic materials. Finally, the presented solution can easily be utilized for transversely isotropic materials or isotropic solids when the constitutive parameters are changed correspondingly.
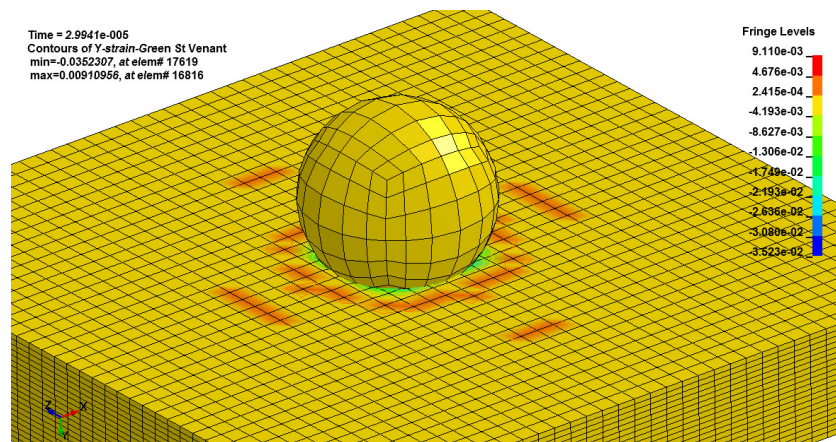
Fig. 10. Normal strain distribution along y axis in the orthotropic cortical bone
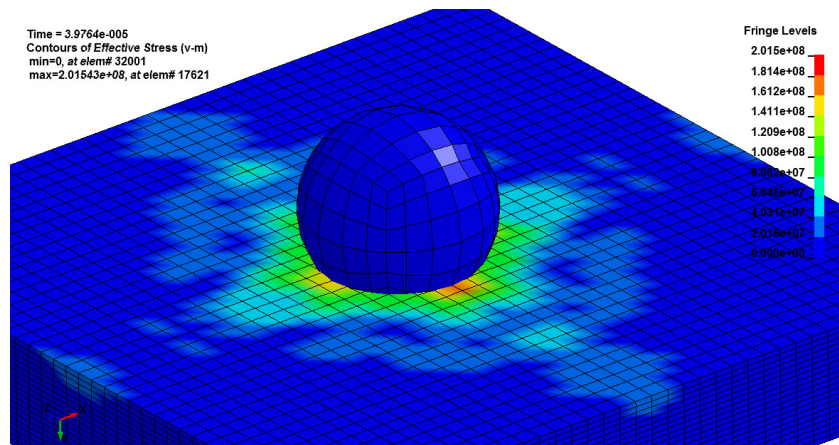

Fig. 11. Von Misses equivalent stress distribution in the orthotropic cortical bone

REFERENCES

1. Lekhnitskii, S., Theory of Elasticity of an Anisotropic Elastic Body, Mir Publishers, Moscow, 1981.

2. Green, A. and Zerna, W., Theoretical Elasticity, Dover Publications, New York, 1992.

3. Popov, V., Contact Mechanics and Friction, Springer–Verlag, Berlin, 2010.

4. Johnson, K. L., Contact Mechanics, Cambridge University Press, New York, 1985.

5. Turner, J., "Contact on a transversely isotropic half-space, or between two transversely isotropic bodies", International Journal of Solids and Structures, 1966, 16, 409–419.

6. Keer, L. and Schonberg, W., "Smooth indentation of a transversely isotropic cantilever beam", International Journal of Solids and Structures, 1986, 22, 1033–1053.

7. Ovaert, T., "On the Indentation of a transversely isotropic half-space with application to thin solid lubricant films", Journal of Applied Mechanics, 1993, 115, 650–657.

8. Brock, L., Georgiadis, H. and Hanson, M., "A rapid indentation of transversely isotropic or orthotropic half-spaces", Journal of Applied Mechanics, 2001, 68, 490–495.

9. Srinivas, S. and Rao, A., "Bending, vibration and buckling of simply supported thick orthotropic rectangular plates and laminates",

International Journal of Solids and Structures, 1970, 6, 1463–1481.

10. Miller, G., "A Green's function solution for plane anisotropic contact problems", Journal of Applied Mechanics, 1986, 53, 386–389.

11. Tan, T. and Sun, C., "Use of statical indentation laws in the impact analysis of laminated composite plates", Journal of Applied Mechanics, 1985, 5, 6–12.

12. Wu, E. and Yen, C., "The contact behavior between laminated composite plates and rigid spheres", Journal of Applied Mechanics, 1994, 61, 60–66.

13. Chao, C. and Tu, C., "Three-dimensional contact dynamics of laminated plates: Part 1. Normal impact", Composites: Part B, 1999, 30, 9–22.

14. Mahajan, P., "Contact behavior of an orthotropic laminated beam indented by a rigid cylinder", Composites Science and Technology, 1998, 58, 505–513.

15. Fan, Z., Swadener, J., Rho, J., Roy, M. and Pharr, G., "Anisotropic properties of human tibial cortical bone as measured by nanoindentation", Journal of Orthopaedic Research, 2002, 20, 806–810.

16. Shi, D., Lin, Y. and Ovaert, T., "Indentation of an orthotropic half-space by a rigid ellipsoidal indenter", Journal of Tribology, 2003, 125, 223–231.

17. Kagadii, T. and Pavlenko, A., "Contact problem for an elastic orthotropic half–strip", International Applied Mechanics, 2003, 39, 1179–1187.

18. Delafargue, A. and Ulm, F., "Explicit approximations of the indentation modulus of elastically orthotropic solids for conical indenters", International Journal of Solids and Structures, 2004, 41, 73519–73560.

19. Swanson, S., "Contact deformation and stress in orthotropic plates", Composites: Part A, 2005, 36, 1421–1429.

20. Willis, J., "Hertzian contact of anisotropic bodies", Journal of the Mechanics and Physics of Solids, 1966, 14, 163–176.

21. Fukumasu, N. and Souza, R., "Numerical analysis of the contact stresses developed during the indentation of coated systems with substrates with orthotropic properties", Surface & Coatings Technology, 2006, 201, 4294–4299.

22. Kowalczyk, P., "Orthotropic properties of cancellous bone modelled as parameterized cellular material", Computer Methods in Biomechanics and Biomedical Engineering, 2006, 9, 135–147.

23. Lovell, M. and Morrow, C., "Three–dimensional contact analysis of anisotropic coated surfaces", Tribology Transactions, 2006, 49, 33–38.

24. Kahya, V., Birinci, A. and Erdol, R., "Frictionless contact problem between two orthotropic elastic layers", International Journal of Computational and Mathematical Sciences, 2007, 1, 121–127.

25. Batra, R. and Jiang, W., "Analytical solution of the contact problem of a rigid indenter and an anisotropic linear elastic layer", International Journal of Solids and Structures, 2008, 45, 5814–5830.

26. Stroh, A., "Steady state problems in anisotropic elasticity", Journal of Mathematics and Physics, 1962, 41, 77–103.

27. Ashrafi, H. and Farid, M., "A computational matrix inversion approach for analysis of contact problems between any rigid nanoindenter and viscoelastic bodies", Mechanical and Aerospace Engineering Journal, 2010, 5, 33–42.

28. Ashrafi, H. and Farid, M., "A new numerical approach for contact analysis between a spherical nanoindenter and the surface of a viscoelastic half–space", Iranian Journal of Surface Science and Technology, 2011, 10, 1–10.

29. Wylie, C. and Barrett, L., Advanced Engineering Mathematics, McGraw–Hill, New York, 1985.

30. Bracewell, R., The Fourier Transform and Its Applications, McGraw–Hill, New York, 1999.

31. Zhong, Z., Finite Element Procedures for Contac – Impact Problems, Oxford University Press, New York, 1993.

32. Laursen, T., Computational Contact and Impact Mechanics, Springer–Verlag, Berlin, 2002.

33. Cowin, S., Bone Mechanics Handbook, Second Edition, CRC Press, New York, 2001.